Supporting Information

A phosphonated poly(ethylenedioxythiophene) derivative with low oxidation potential for energy-efficient bioelectronic devices

Jonathan Hopkins,[1] Kristina Fidanovski,[1] Lorenzo Travaglini,[1] Daniel Ta,[2] James Hook,[3] Pawel Wagner,[4] Klaudia Wagner,[4] Antonio Lauto,[2] Claudio Cazorla,[5] David Officer,[4] Damia Mawad[1,6]*

[1] School of Materials Science and Engineering, UNSW Sydney, Sydney, New South Wales 2052, Australia

[2] School of Science, Western Sydney University, Locked Bag 1797, Penrith, NSW 2751, Australia

[3] School of Chemistry, University of New South Wales, Sydney, NSW, 2052, Australia

[4] Intelligent Polymer Research Institute and ARC Centre of Excellence for Electromaterials Science, University of Wollongong, New South Wales 2522, Australia

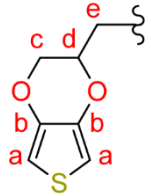[5] Departament de Física, Universitat Politècnica de Catalunya, Campus Nord B4-B5, Barcelona 08034, Spain
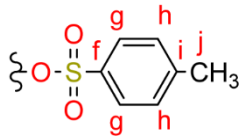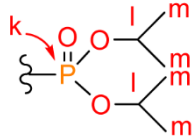
[6] Australian Centre for NanoMedicine, UNSW Sydney, Sydney, New South Wales 2052, Australia

Table of Contents

1 Nuclear magnetic resonance (NMR) spectroscopy

Table S1. Summary of results from one-dimensional NMR spectra of monomers. Three dashes (---) denote environments with no expected peaks. The NMR spectra of monomers and the polymer PEDOT-Phos are also presented in the following figures (Figure S1 to Figure S13).

Environment	Chemical shift (δ, ppm) and signal characteristics						
	EDOT-Tos		**EDOT-I**		**EDOT-Phos**		
	^{1}H	^{13}C	^{1}H	^{13}C	^{1}H	^{13}C	^{31}P
a	6.32 & 6.26 (dd, 2H)	100.2	6.36 (dd, 2H)	100.1 & 100.0	6.32 (dd, 2H)	99.9 & 99.7	---
b	---	140.9 & 140.4	---	141.1 & 140.8	---	141.2 & 141.2	---
c	4.18 (dd, 1H) & 4.03 (dd, 1H)	65.0	4.31 (dd, 1H) & 4.15 (dd, 1H)	67.3	4.35 (dd, 1H) & 3.97 (dd, 1H)	68.0 & 68.0	---
d	4.36 (m, 1H)	70.8	4.26 (m, 1H)	72.9	4.49 (m, 1H)	69.4	---
e	4.22 (m, 2H)	66.9	3.33 (m, 2H)	0.7	2.20 (dd, 1H) & 2.06 (dd, 1H)	30.3 & 28.9	---
f	---	145.3	---	---	---	---	---
g	7.80 (d, 2H)	128.1	---	---	---	---	---
h	7.36 (d, 2H)	130.0	---	---	---	---	---
i	---	132.4	---	---	---	---	---
j	2.46 (s, 3H)	21.7	---	---	---	---	---
k	---	---	---	---	---	---	23.3
l	---	---	---	---	4.75 (m, 2H)	70.8	---
m	---	---	---	---	1.34 (dd, 12H)	24.0	---
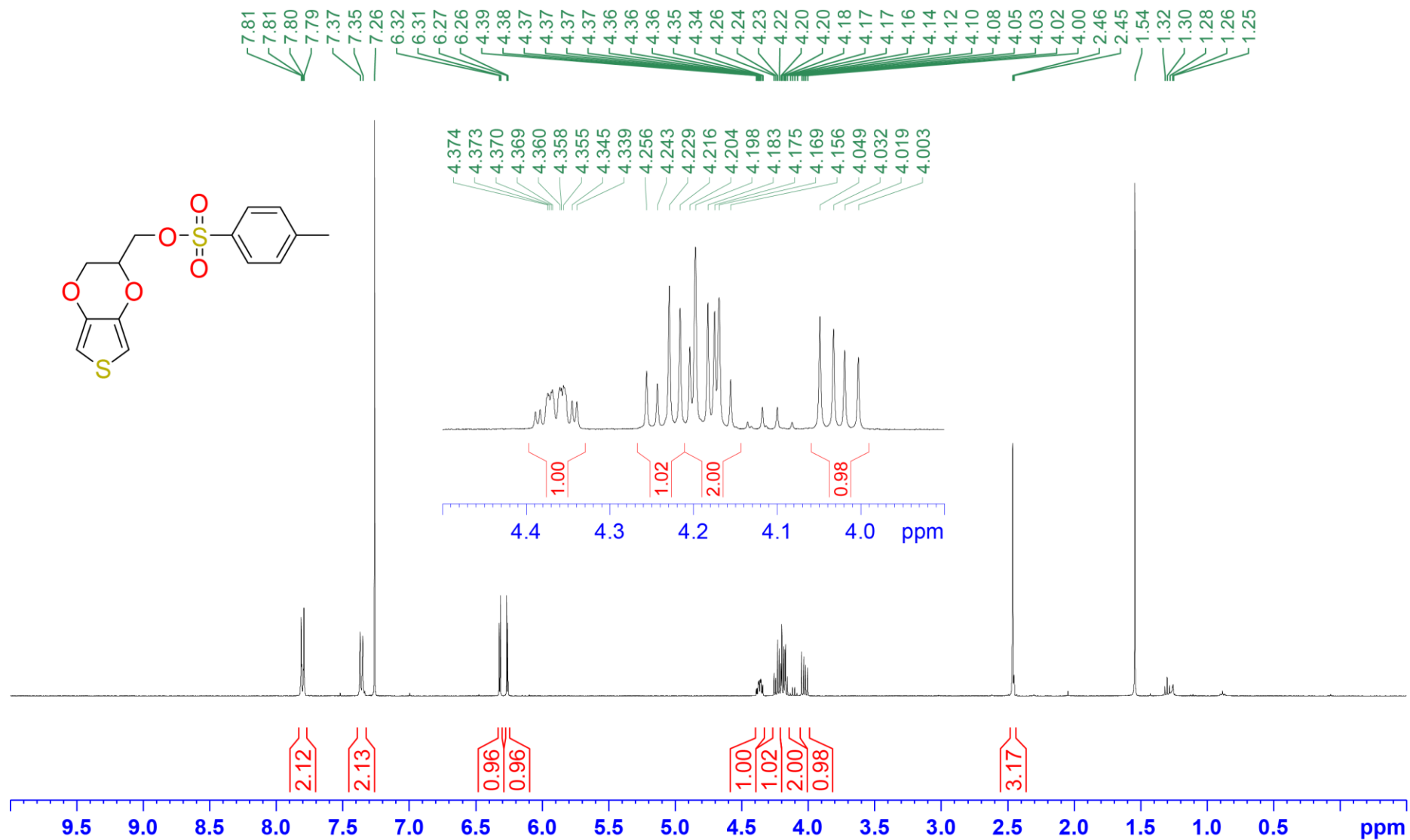
Figure S1. ^{1}H-NMR (400 MHz, CDCl$_3$) spectrum of EDOT-Tos.
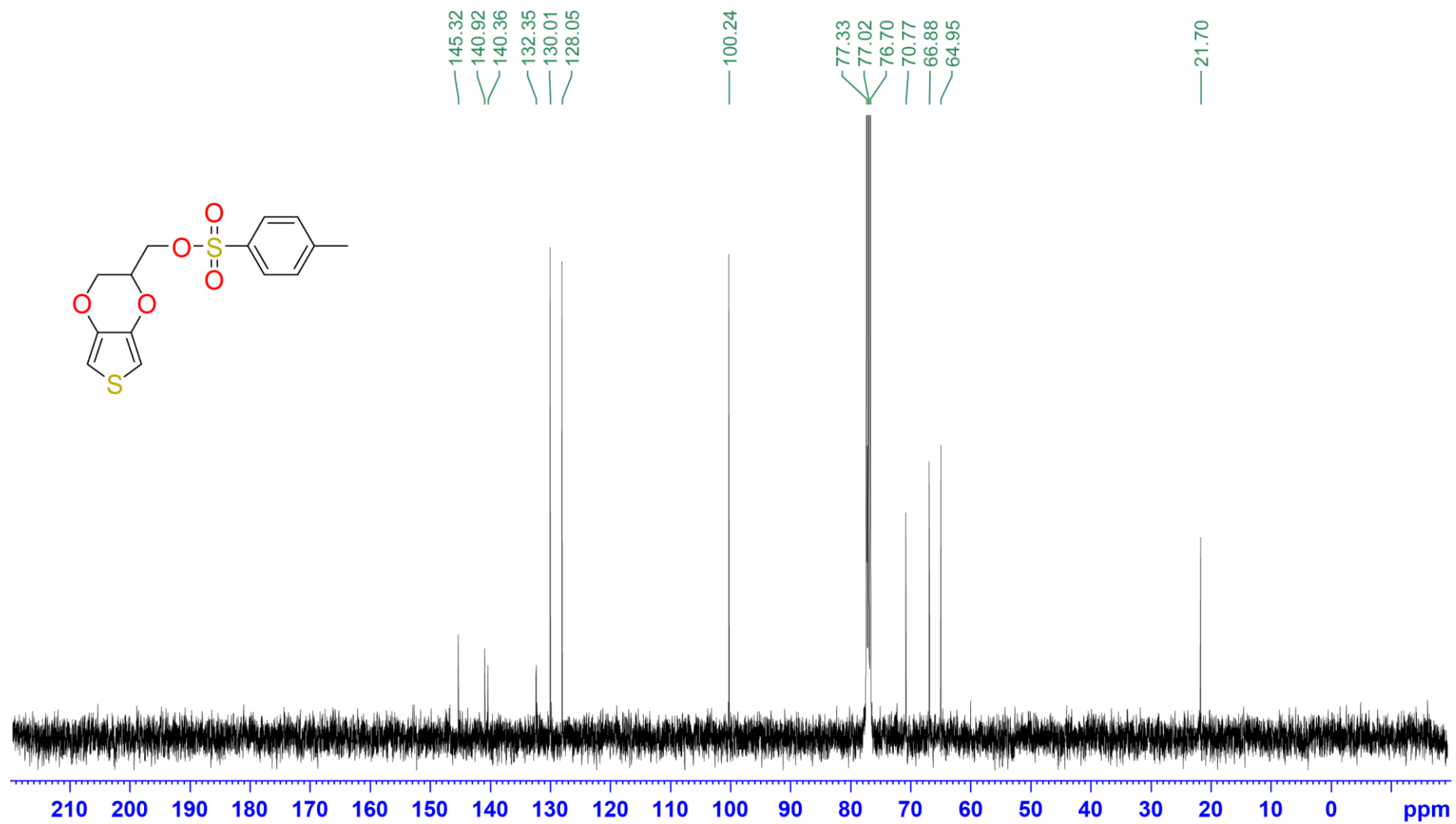
Figure S2. ^{13}C-NMR (100 MHz, CDCl$_3$) spectrum of EDOT-Tos.
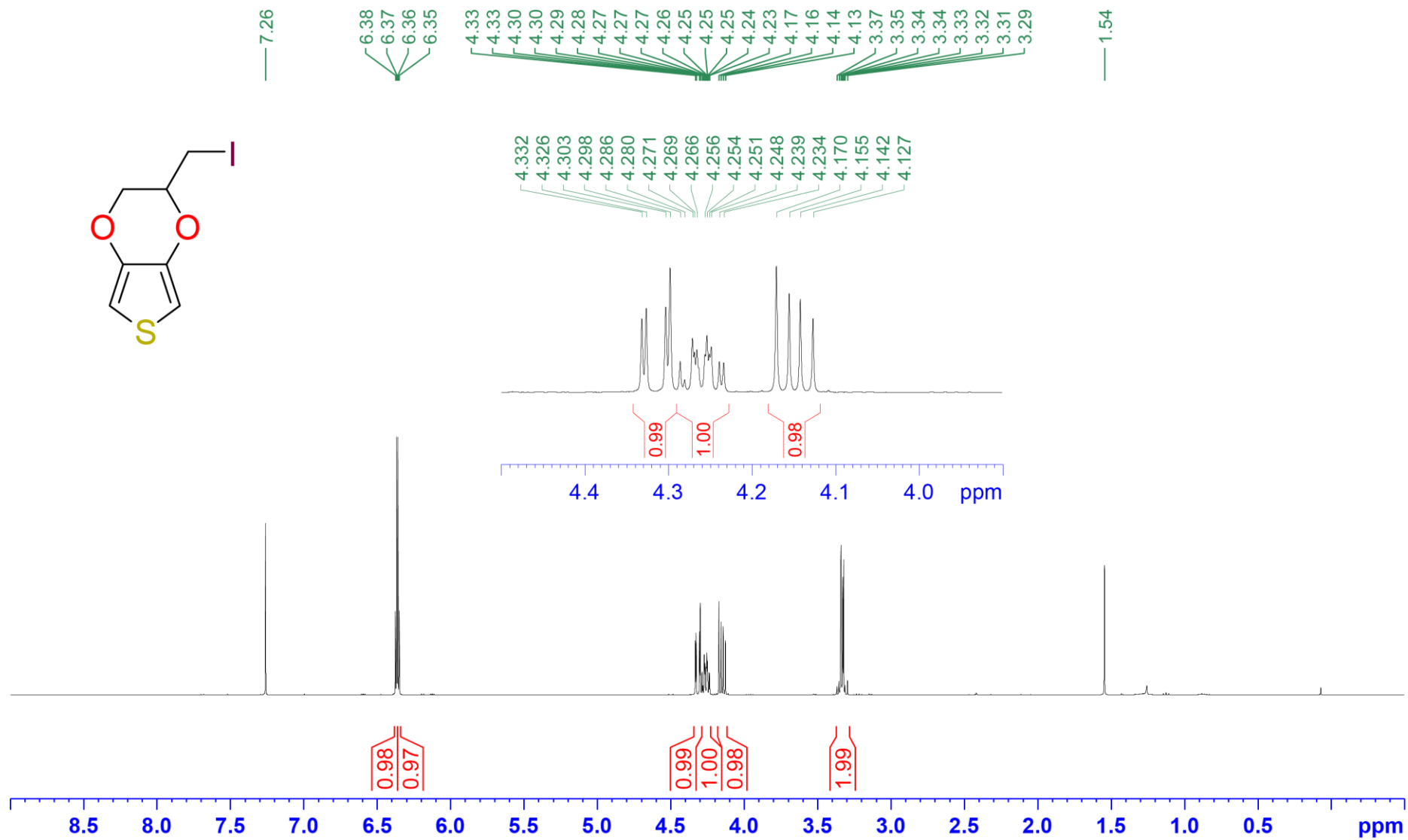
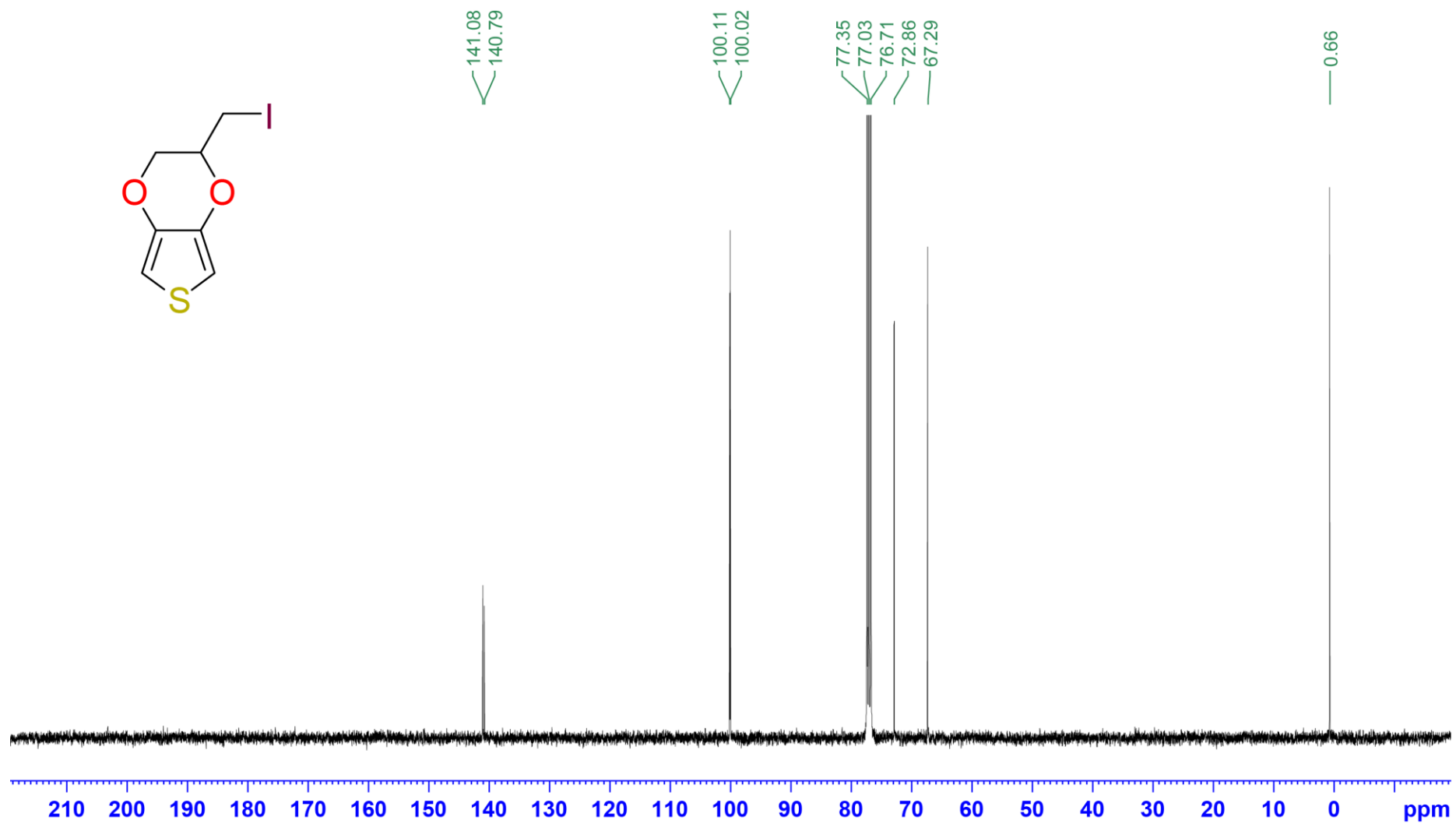**Figure S3.** ^{1}H-NMR (400 MHz, CDCl$_3$) spectrum of EDOT-I.

Figure S4. ^{13}C-NMR (100 MHz, CDCl$_3$) spectrum of EDOT-I.
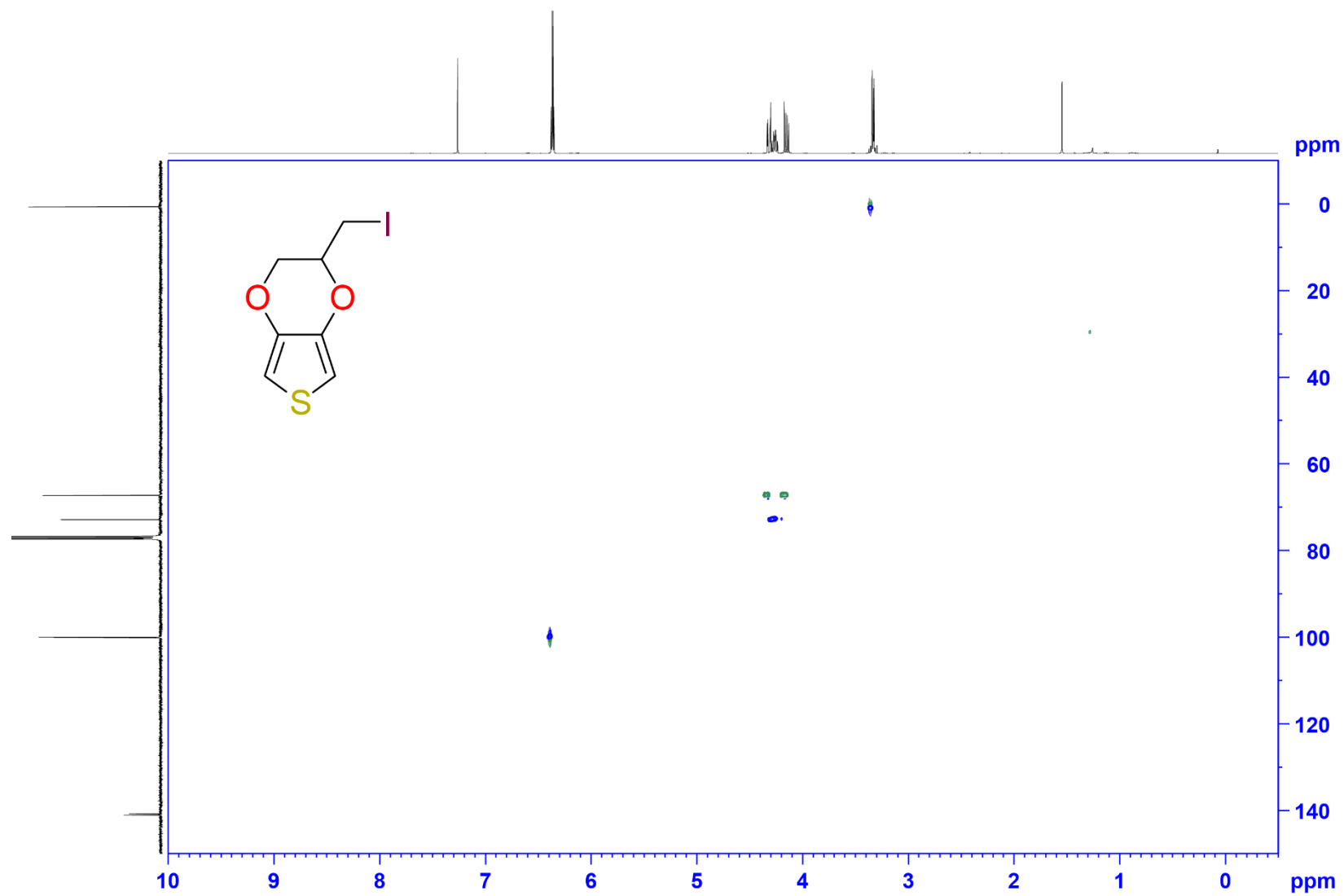
Figure S5. ^1H-^{13}C HSQC NMR (CDCl$_3$) spectrum of EDOT-I.
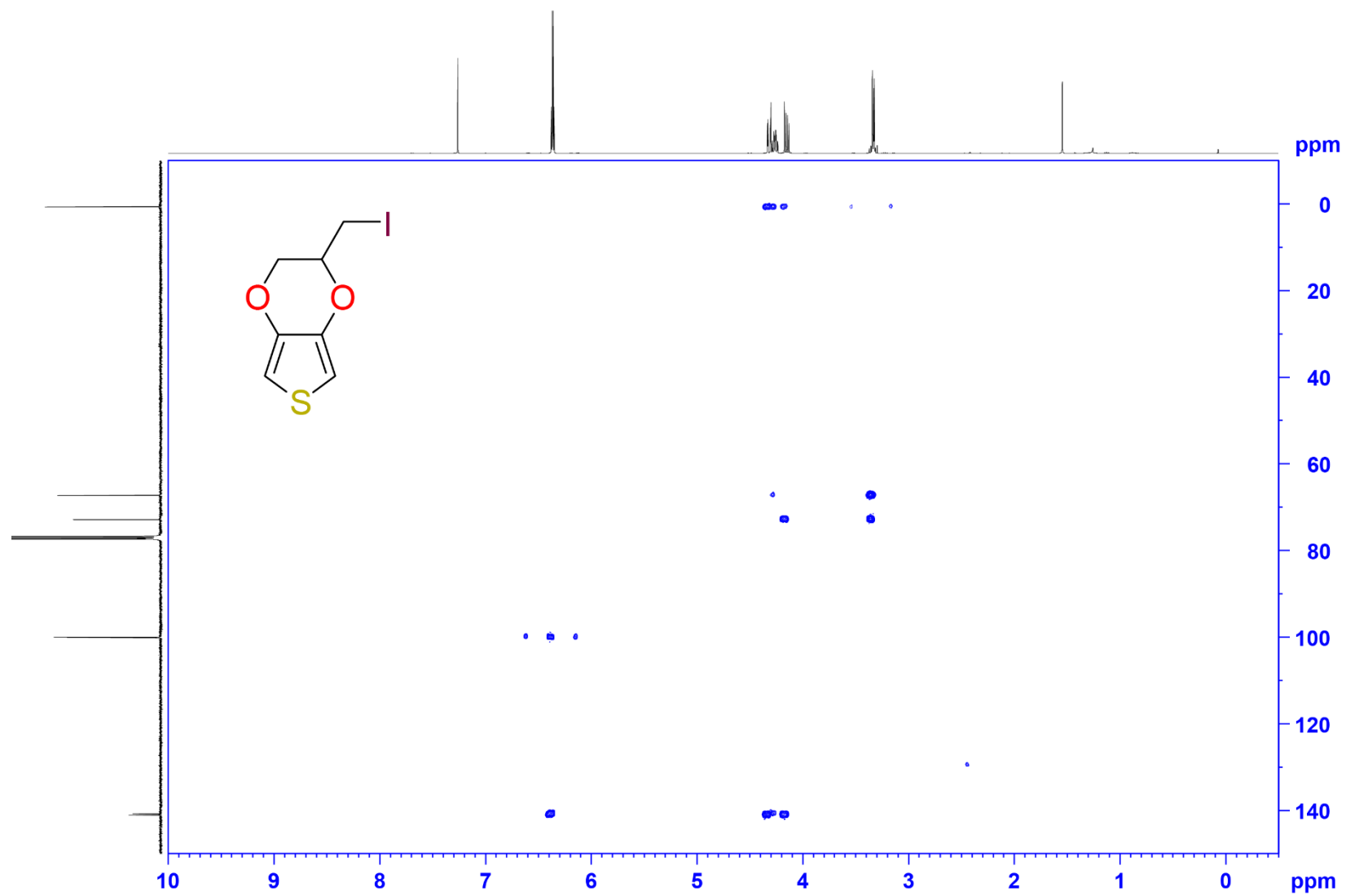
Figure S6. ^{1}H-^{13}C HMBC NMR (CDCl$_3$) spectrum of EDOT-I.

Figure S7. ^{1}H-NMR (400 MHz, CDCl$_3$) spectrum of EDOT-Phos.
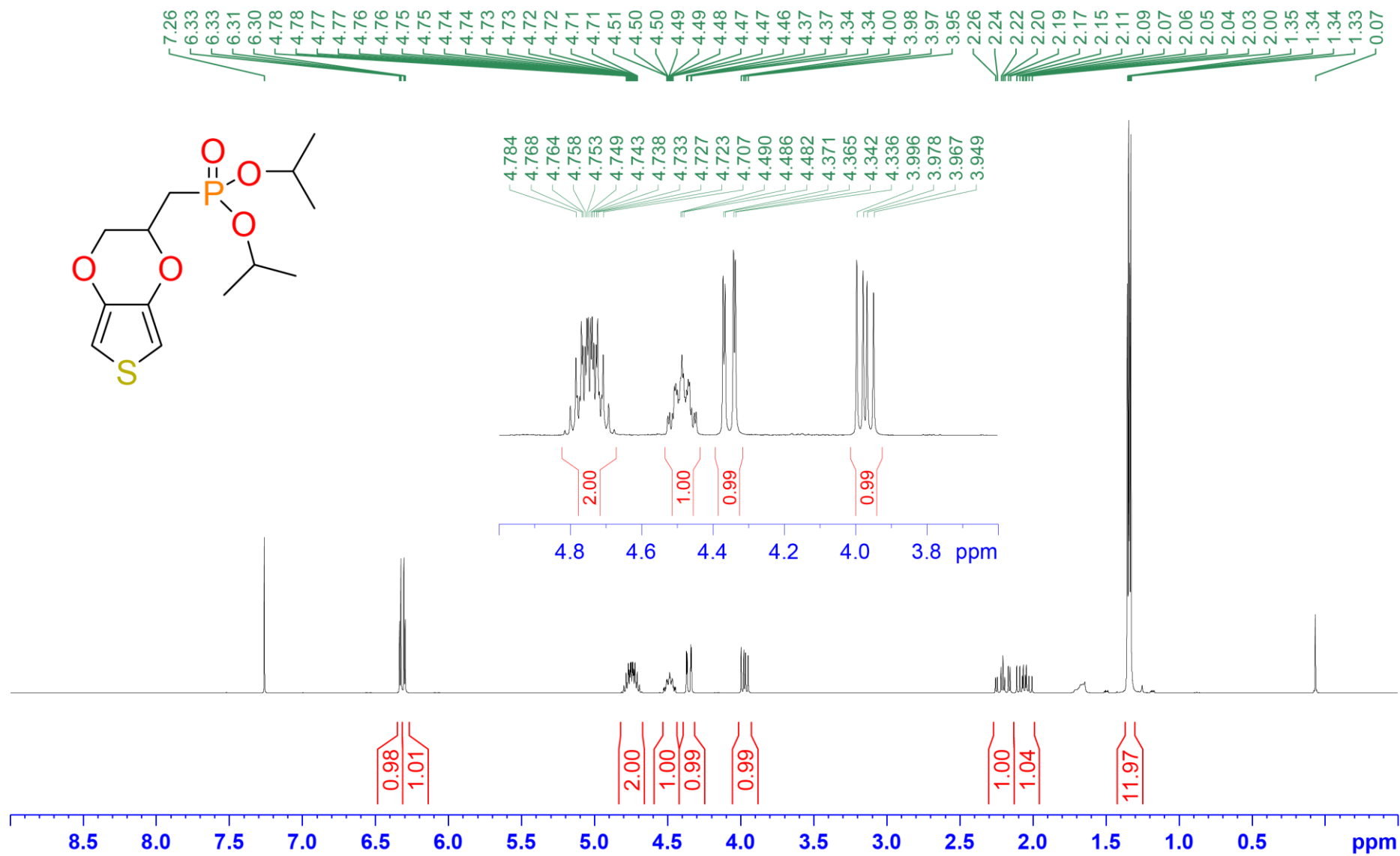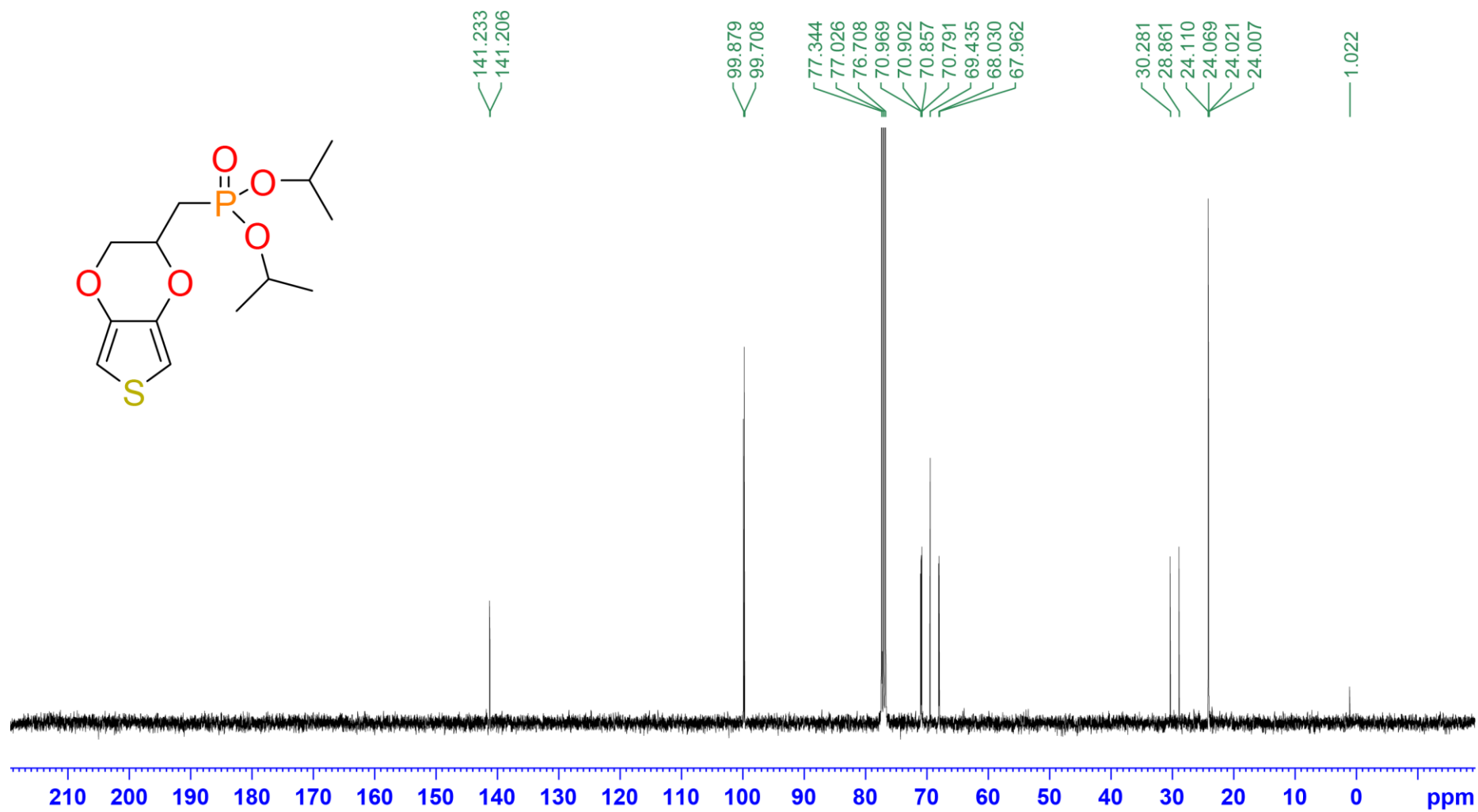
Figure S8. ^{13}C-NMR (100 MHz, CDCl$_3$) spectrum of EDOT-Phos.
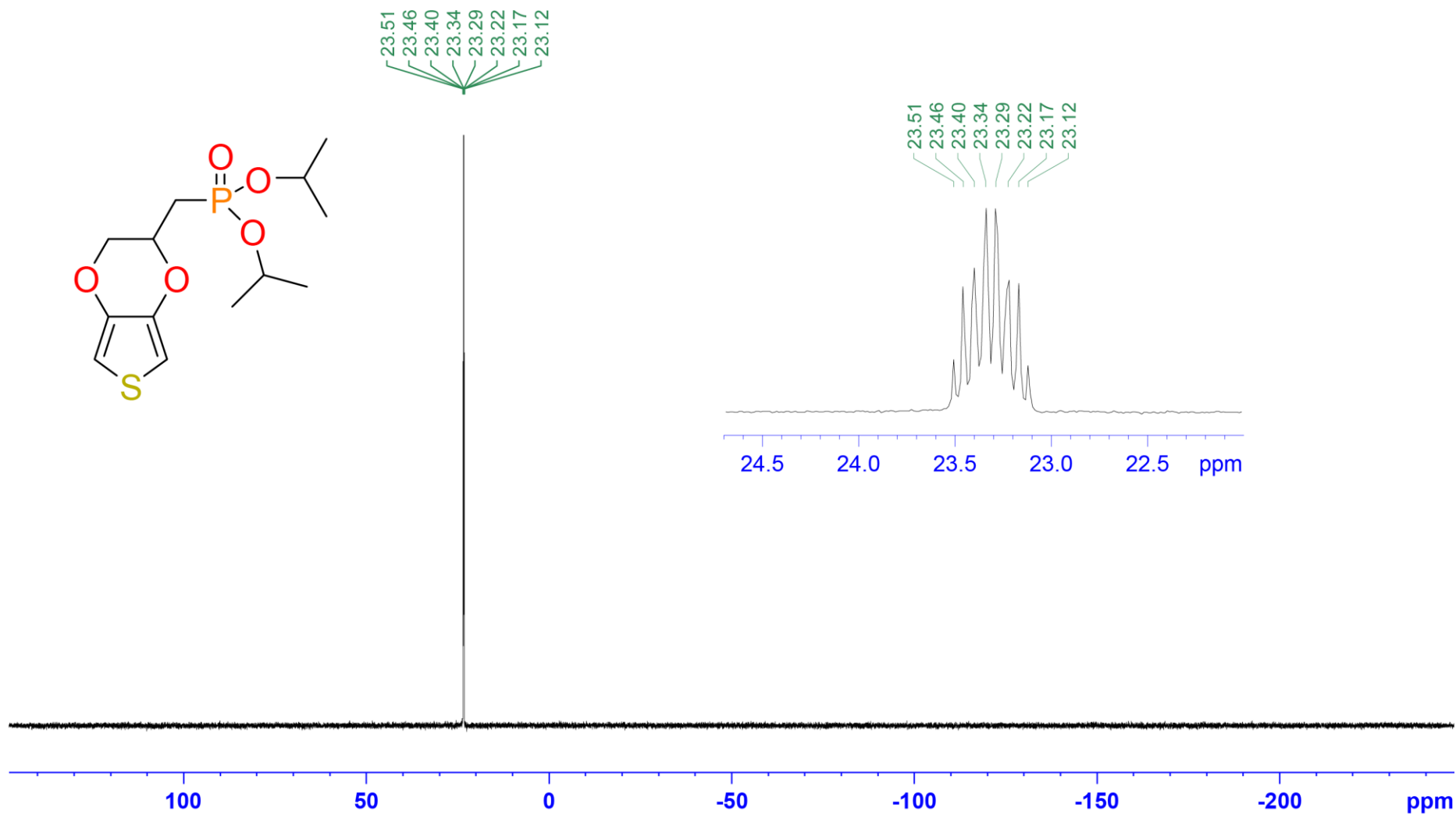
Figure S9. ^{31}P-NMR (162 MHz, CDCl$_3$) spectrum of EDOT-Phos.
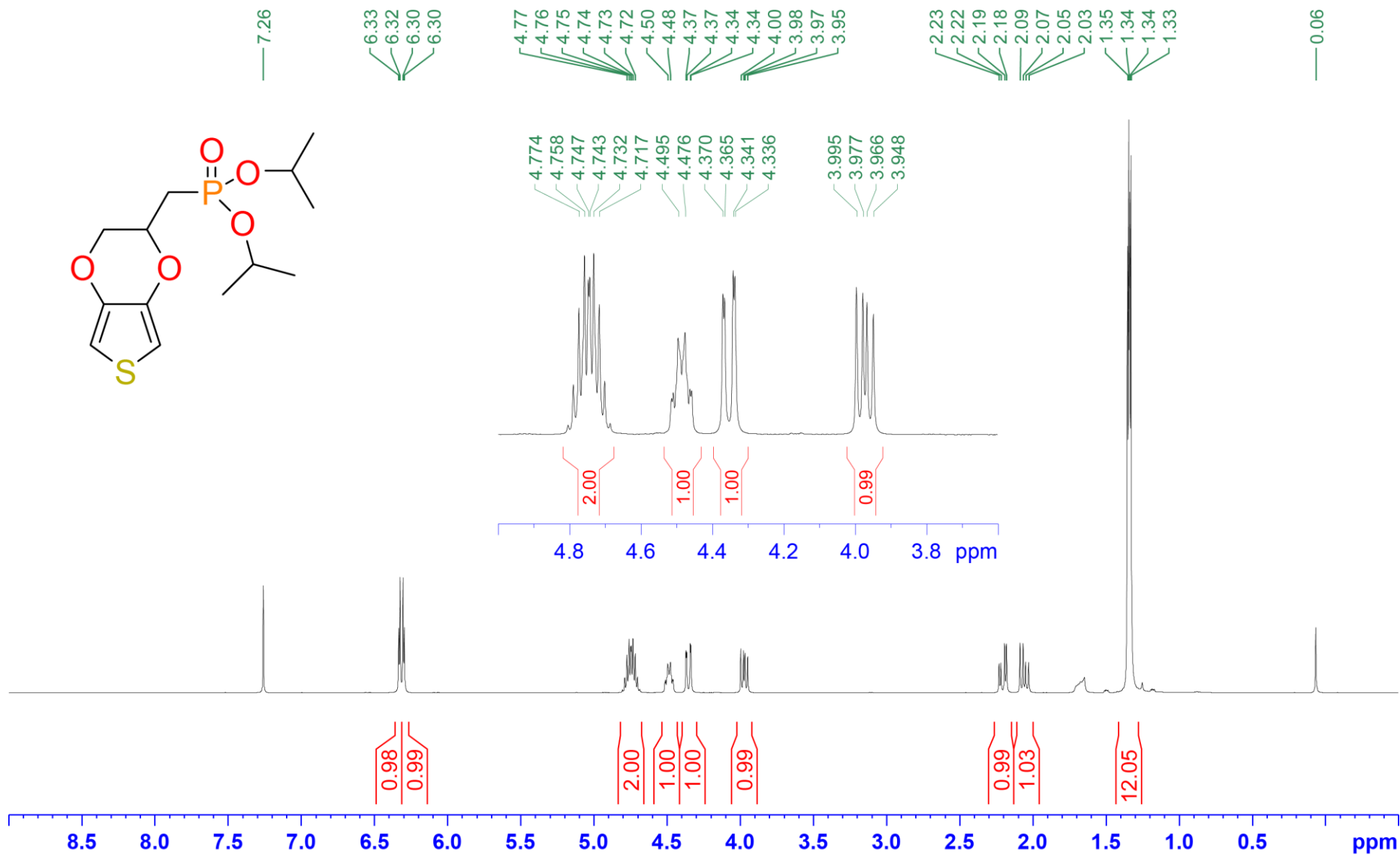
Figure S10. $^1H\{^{31}P\}$-NMR (400 MHz, CDCl$_3$) decoupled spectrum of EDOT-Phos.
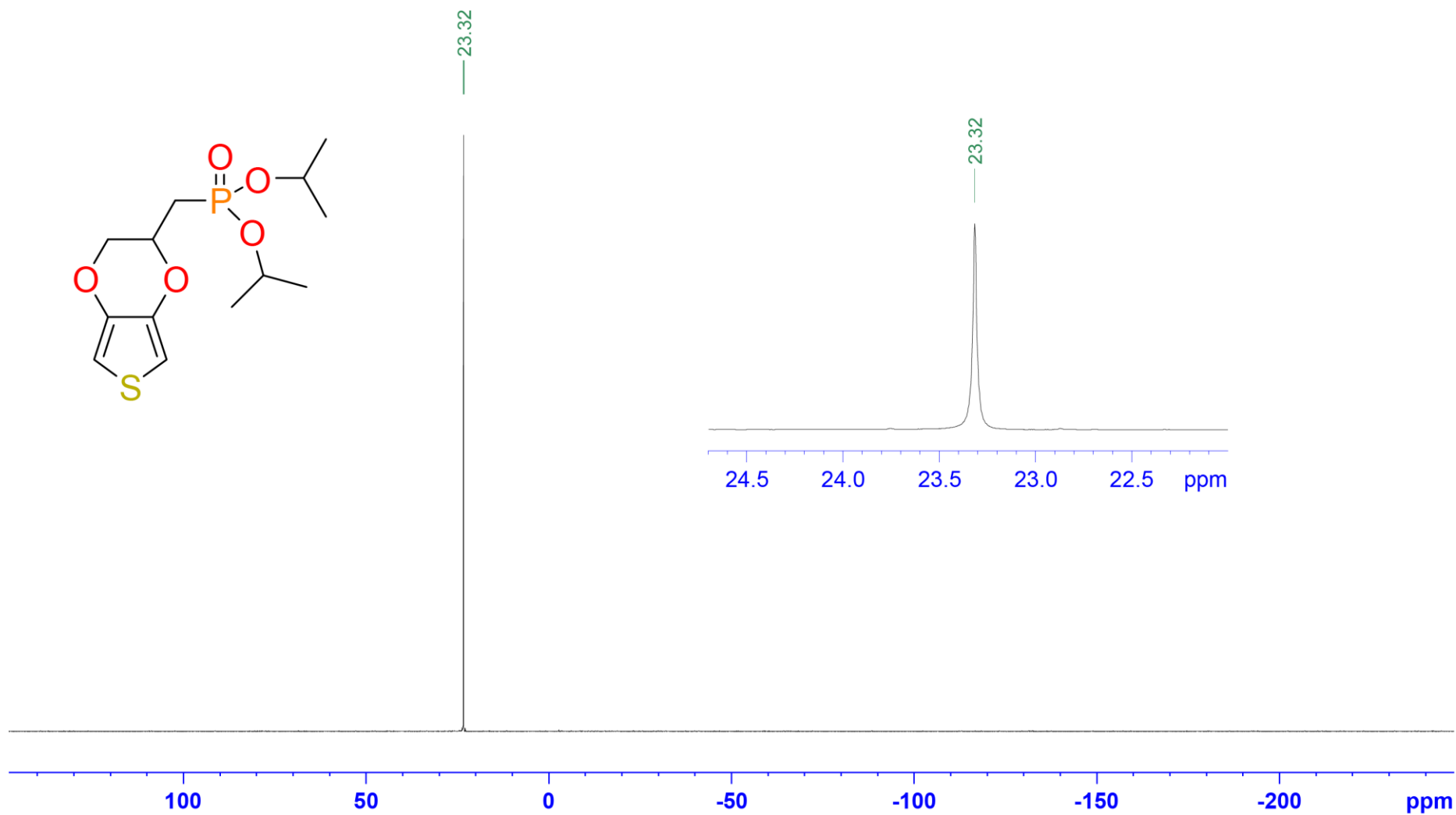
Figure S11. $^{31}P\{^1H\}$-NMR (162 MHz, CDCl$_3$) decoupled spectrum of EDOT-Phos.
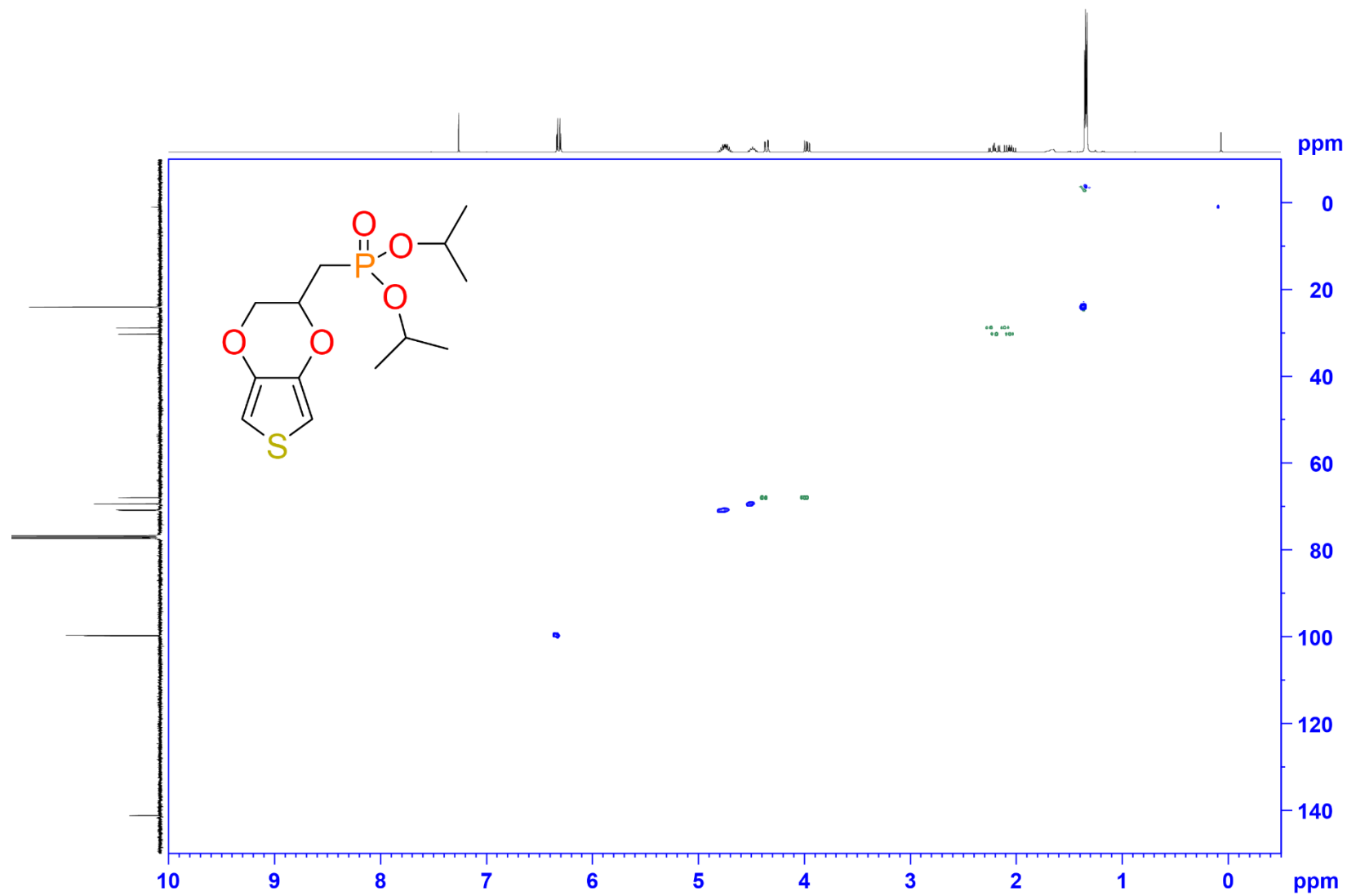
Figure S12. ^1H-^{13}C HSQC NMR (CDCl$_3$) spectrum of EDOT-Phos.
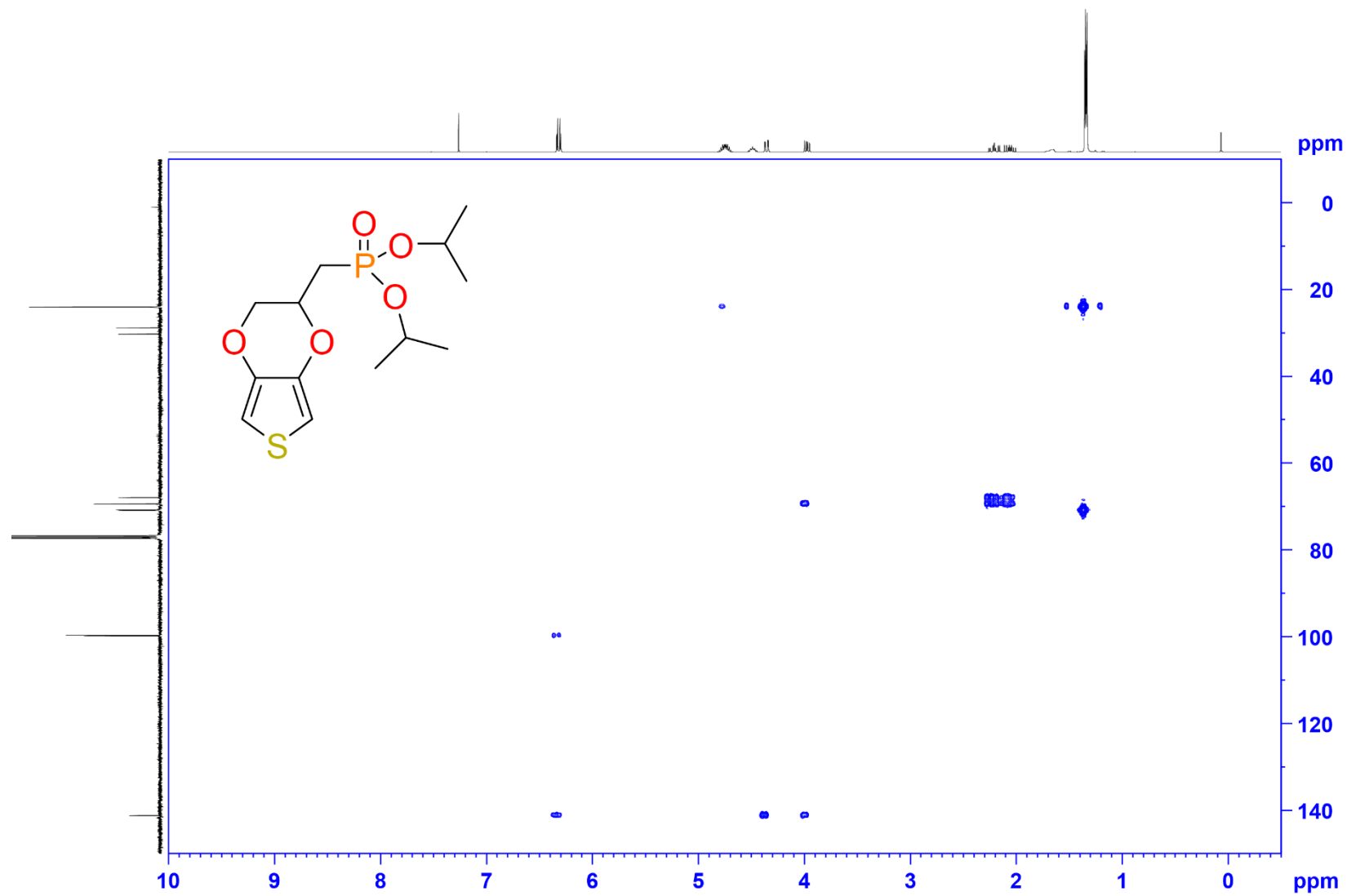
Figure S13. ^{1}H-^{13}C HMBC NMR (CDCl$_3$) spectrum of EDOT-Phos.

2 Structural characterisation
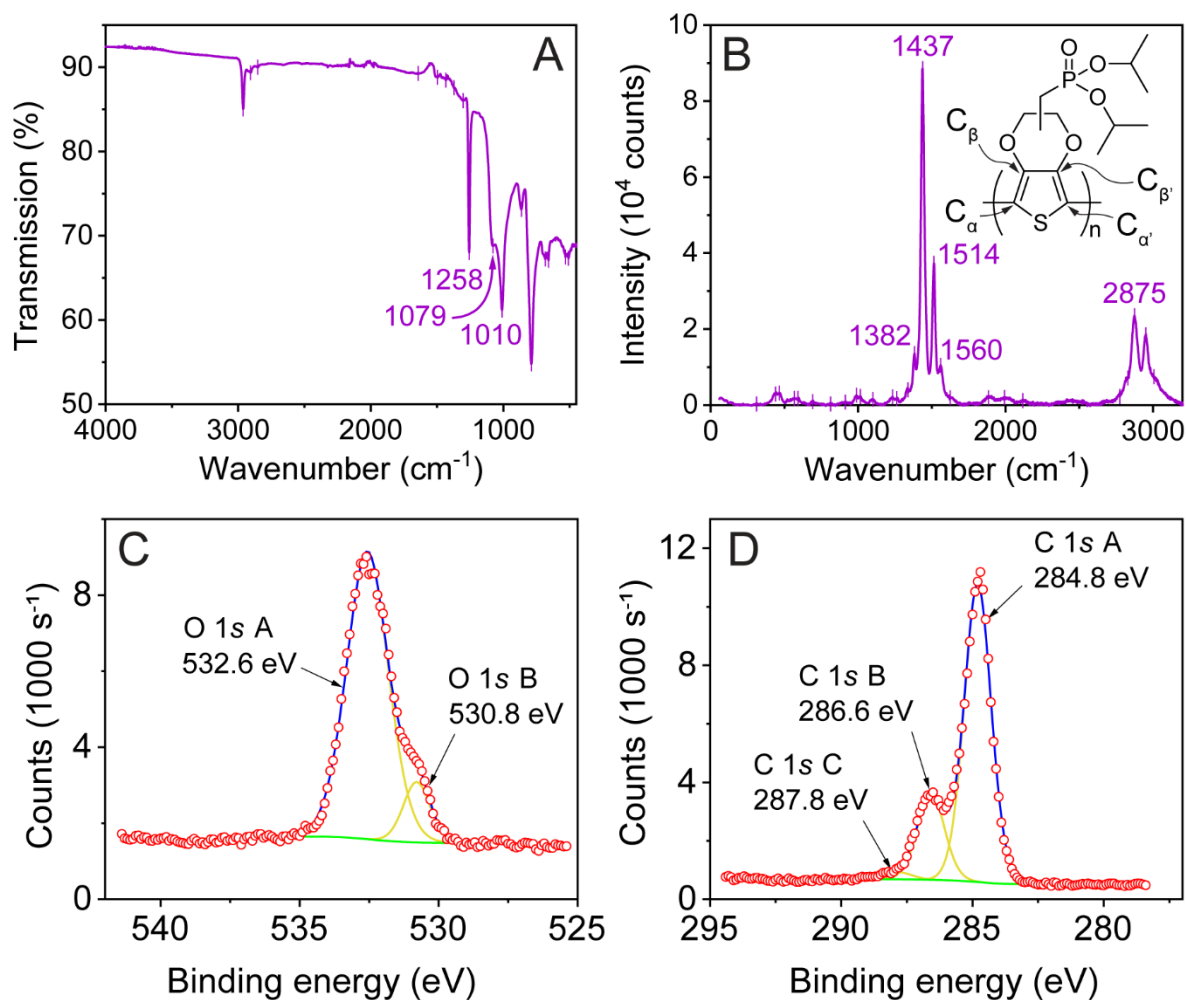
Figure S14. (A) Full, normalised ATR-FTIR spectrum and (B) laser Raman spectrum (532 nm) of PEDOT-Phos film on ITO. The inset of (B) shows the chemical structure of PEDOT-Phos with the α- and β-carbon atoms labelled. (C-D) XPS spectra of PEDOT-Phos/ITO film showing the (C) O 1s and (D) C 1s environments.

Table S2. Assignment of peaks observed in ATR-FTIR and Raman spectroscopy of PEDOT-Phos/ITO films. C_α and C_β refer to the α- and β-carbon atoms of PEDOT-Phos in the labelled structure of Figure S14B.

| Description	ATR-FTIR (cm^{-1})	Raman (cm^{-1})	References
Aliphatic CH_2 stretch	---	3007	[1,2]
Aliphatic CH_2/CH_3 stretch	2963	2950	[1,2]
Aliphatic CH_2/CH_3 stretch	2908	2875	[1,2]
Aliphatic CH_2 stretch	2854	2830	[1,2]
Aliphatic CH_2 bend	---	1560	[2]
Asymmetric $C_\alpha=C_\beta$ stretch	1497	1514	[1,2]
Symmetric $C_\alpha=C_\beta$(-O) stretch	1434	1437	[1]
Thiophene C_β–C_β stretch	1372	1382	[1,2]
Aliphatic CH_2 twist	1303	1337	[2]
$C_\alpha=C_{\alpha'}$ inter-ring stretch	---	1261	[1,3]
Phosphonate P=O stretch	1258	---	[4]
$C_\alpha=C_{\alpha'}$ inter-ring stretch	---	1233	[1,2]
C-O-C deform	---	1100	[1]
Phosphonate O-P-O stretch + C-O-C deform	1079	---	[1,4,5]
Ethylenedioxy ring deform	---	1015	[2]
Phosphonate P-O(-C) stretch + C-O stretch	1010	---	[2,4,5]
Ethylenedioxy ring deform	---	989	[2]
Phosphonate (C-)P-O stretch	864	913	[4,5]
Ethylenedioxy ring deform	789	814	[1,2]
Ethylenedioxy CH_2 rocking	703	---	[2]
Symmetric C-S-C deform	683	692	[2]
Ethylenedioxy ring deform	---	568	[1,2]
C-O-C deform	---	440	[1,2]

3   *Optical, electrochemical, theoretical, and morphological properties*
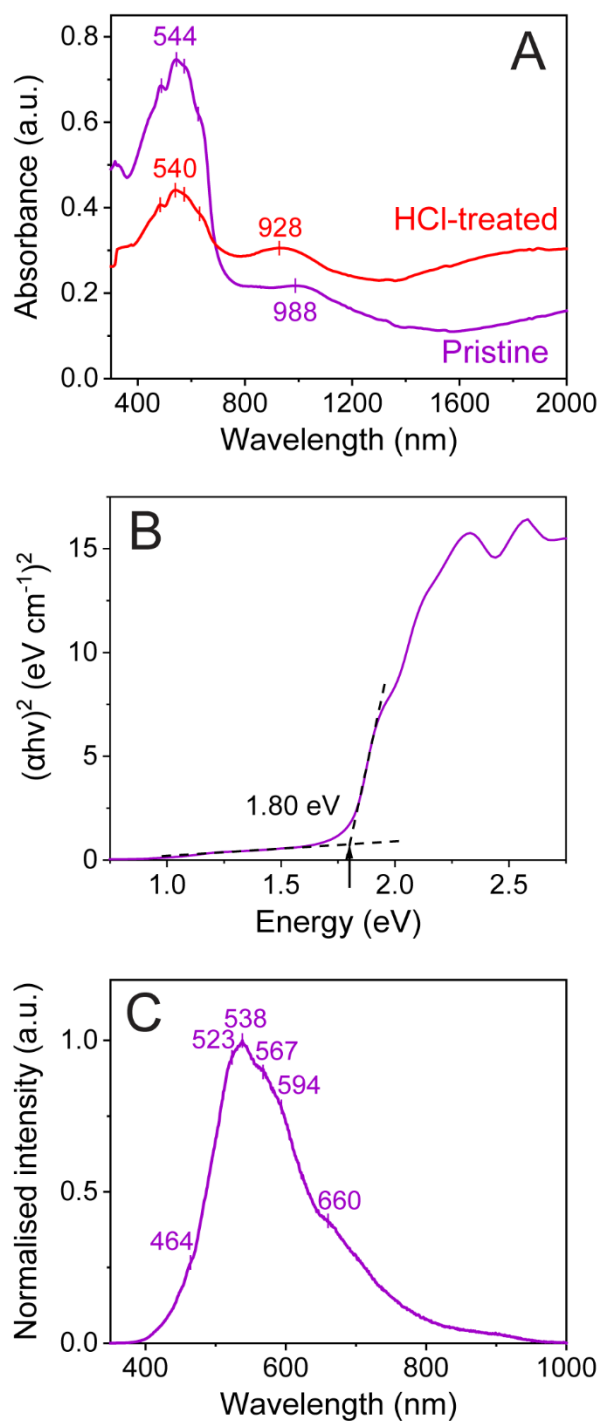

Figure S15. (A) UV-vis-NIR absorbance spectra of PEDOT-Phos films on glass, before and after treatment with HCl (10 μL dropped on the film surface). (B) Tauc plot of the pristine film in (A), with the optical band gap energy indicated. (C) Photoluminescence spectrum of a PEDOT-Phos film on ITO, at laser wavelength 325 nm.
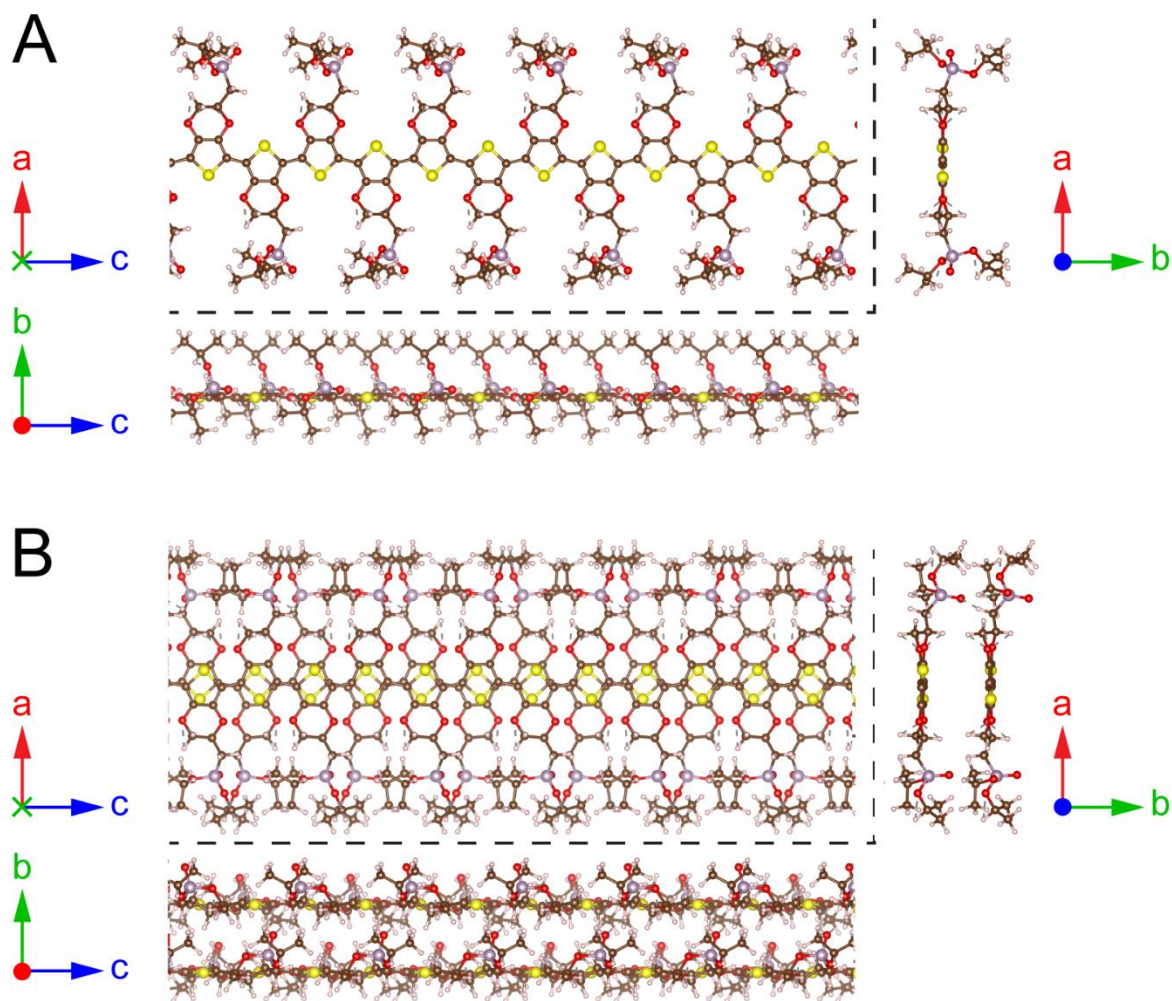
Figure S16. Geometry-optimised molecular models of PEDOT-Phos as (A) a single molecule; (B) a crystalline solid. Atoms are C (brown), H (white), O (red), P (purple), S (yellow).

Table S3. Summary of DFT-calculated and experimental electronic properties of PEDOT-Phos. The HOMO and LUMO energies (E_{HOMO} and E_{LUMO}) are reported relative to the vacuum energy, $E_{vac} = 0$ eV. For the calculated (DFT) case, the bandgap energy was taken as $2 \times E_g$ when calculating the other energies, as described in the Experimental section. The experimental bandgap is the optical bandgap, $E_{g,opt}$, calculated using UV-vis-NIR spectroscopy.

System	E_g (eV)	E_{HOMO} (eV)	E_{LUMO} (eV)	IP (eV)
Calculated	0.79	−4.66	−3.07	4.66
Experimental	1.80	−4.74	−2.95	4.74

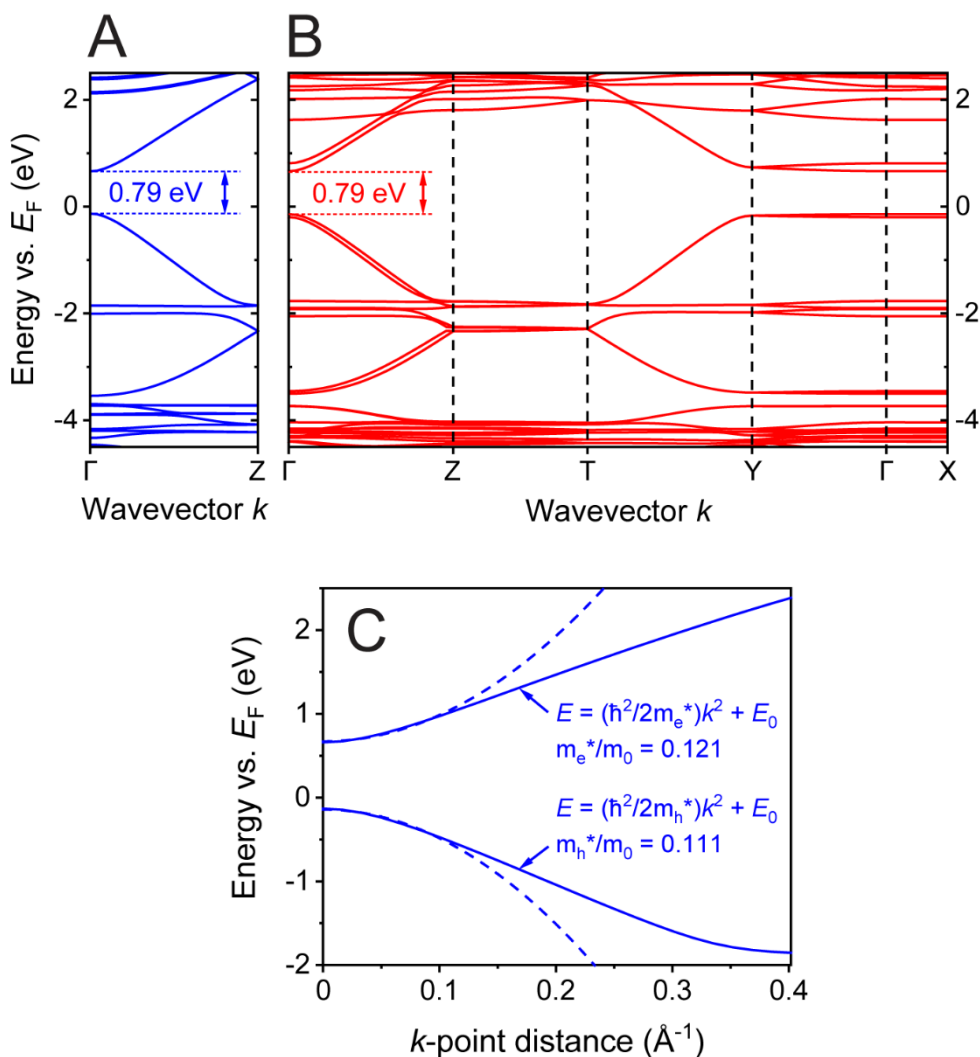**Figure S17.** DFT characterisation of PEDOT-Phos. (A-B) Band structures of (A) an isolated PEDOT-Phos molecule and (B) a PEDOT-Phos crystal, close to the Fermi level (E_F = 0 eV). The high-symmetry points indicated in the band structure are Γ = (0, 0, 0), Z = (0, 0, 0.5), T = (0, 0.5, 0.5), Y = (0, 0.5, 0), X = (0.5, 0, 0). The theoretical direct bandgap is taken from the band structure as E_g = 0.79 eV. (C) Calculation of effective masses of electronic charge carriers at the conduction and valence band edges in the isolated molecule. The conduction and valence bands were each fitted to a parabola in the region close to zero k-point distance, according to the equation $E = (\hbar^2/2m^*)k^2 + E_0$ where E = energy, E_0 = energy at zero k-point distance, $\hbar$ = Planck's constant, m^* = effective mass of holes (valence band) or electrons (conduction band), and k = the k-point distance. The calculated effective masses are indicated on the figure: m_h^*/m_0 = 0.111, m_e^*/m_0 = 0.121.
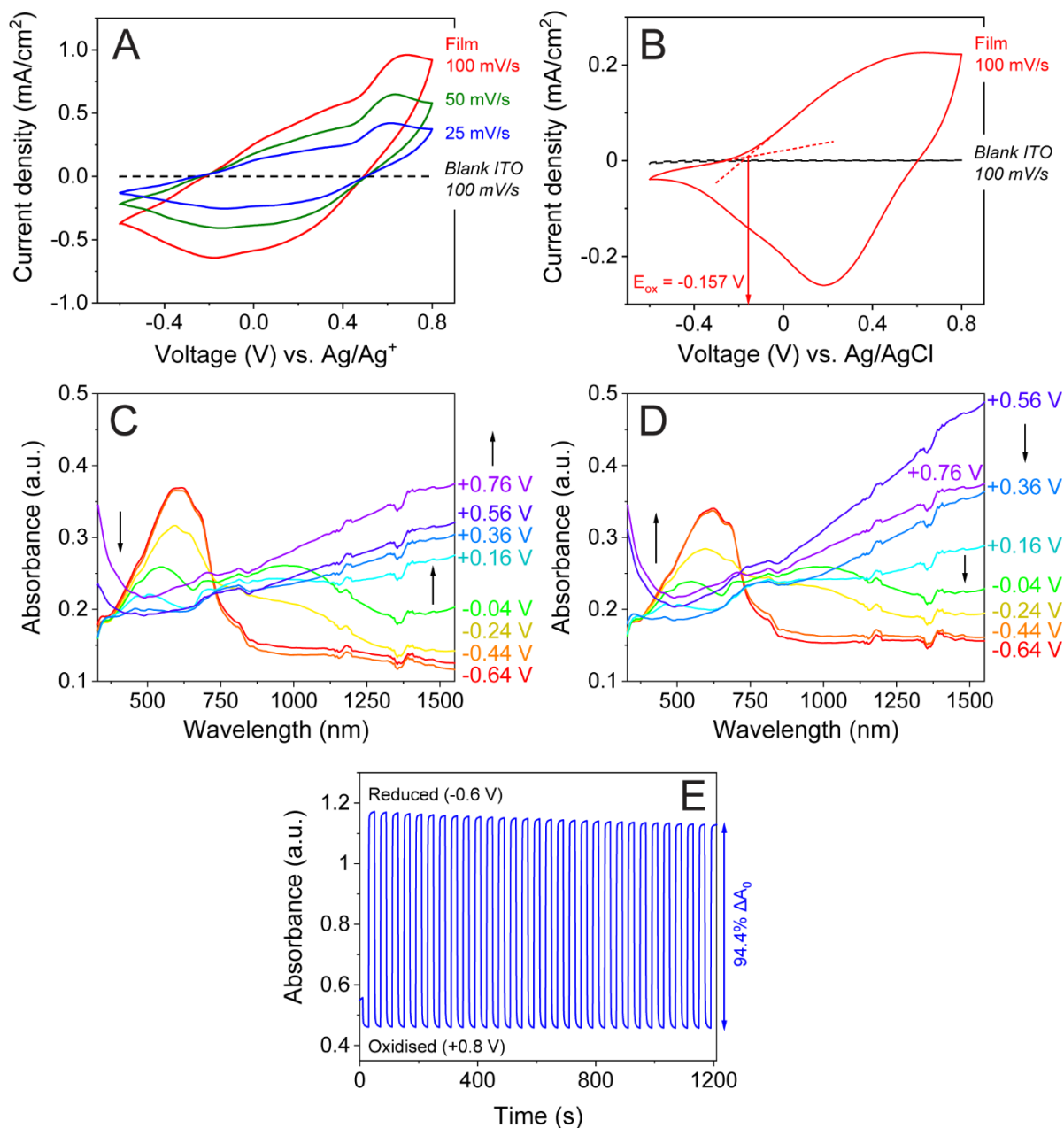
Figure S18. (A) Cyclic voltammetry of PEDOT-Phos on ITO in TBABF$_4$ (0.1 M in CH$_3$CN) at various scan rates over the potential range –0.6 V to +0.8 V. The film was first subjected to 20 relaxation cycles (scan rate 100 mV/s, potential range –0.6 V to +0.8 V) to ensure a stable output. (B) Cyclic voltammetry of PEDOT-Phos on ITO in aqueous NaCl (0.1 M) at 100 mV/s over the potential range –0.6 V to +0.8 V, showing the oxidation onset potential (E$_{ox}$ = –0.157 eV). (C-D) *In-situ* UV-vis-NIR spectroelectrochemistry of PEDOT-Phos/ITO film on ITO in TBABF$_4$ (0.1 M in CH$_3$CN), with (C) increasing and (D) decreasing potential. The potentials were originally recorded vs. Ag wire and are here reported relative to Ag/AgCl (= Ag wire – 0.34 V). (E) Absorbance-time profile at 560 nm for switching of a PEDOT-Phos/ITO film in aqueous NaCl (0.1 M). The final absorbance contrast is labelled relative to the original absorbance contrast, ΔA_0.
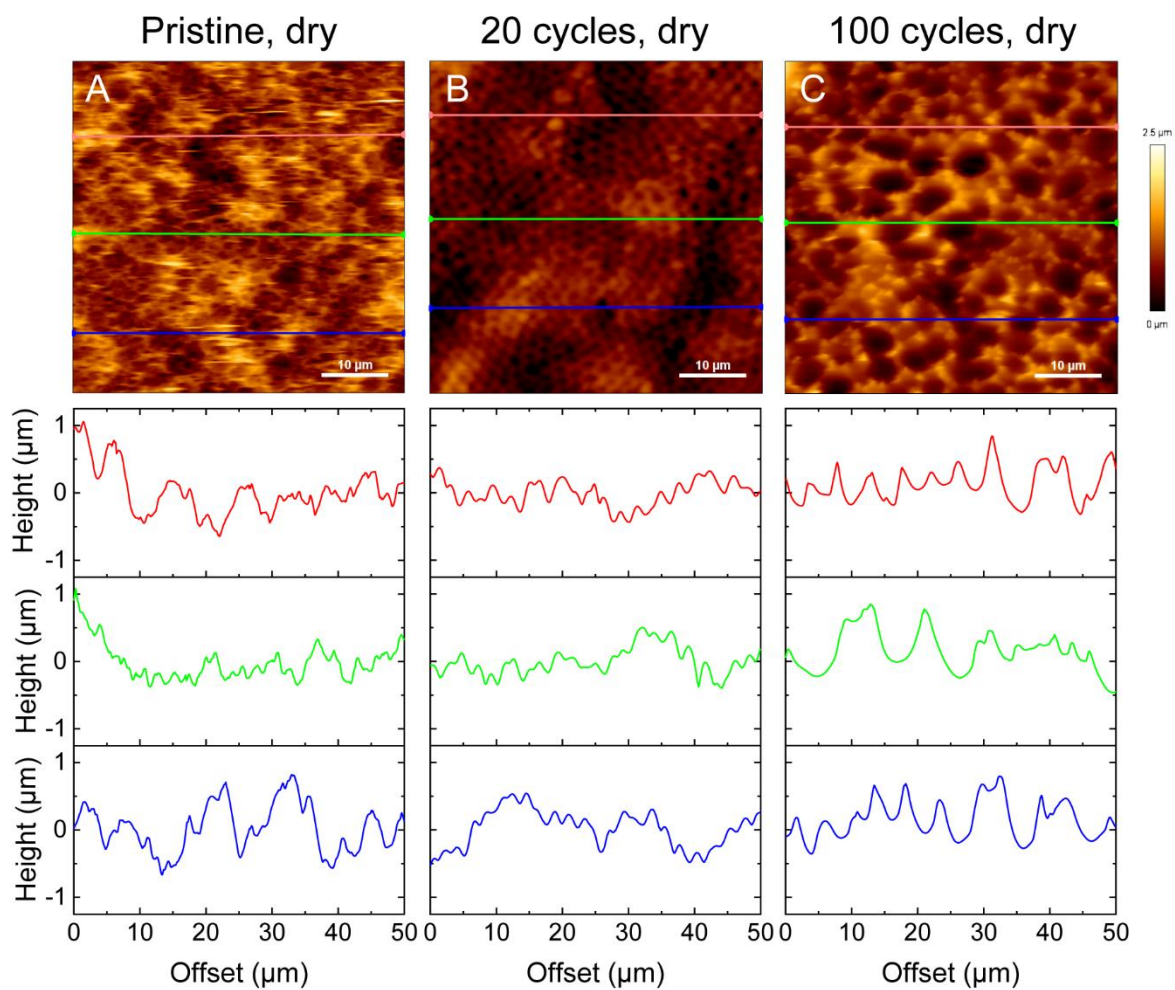
Figure S19. AFM micrographs of dry PEDOT-Phos films on ITO (A) before CV and after (B) 20 cycles and (C) 100 cycles of CV in aqueous NaCl (0.1 M). Height profiles are given for each micrograph along the three marked lines. Scan area: 50 × 50 μm.
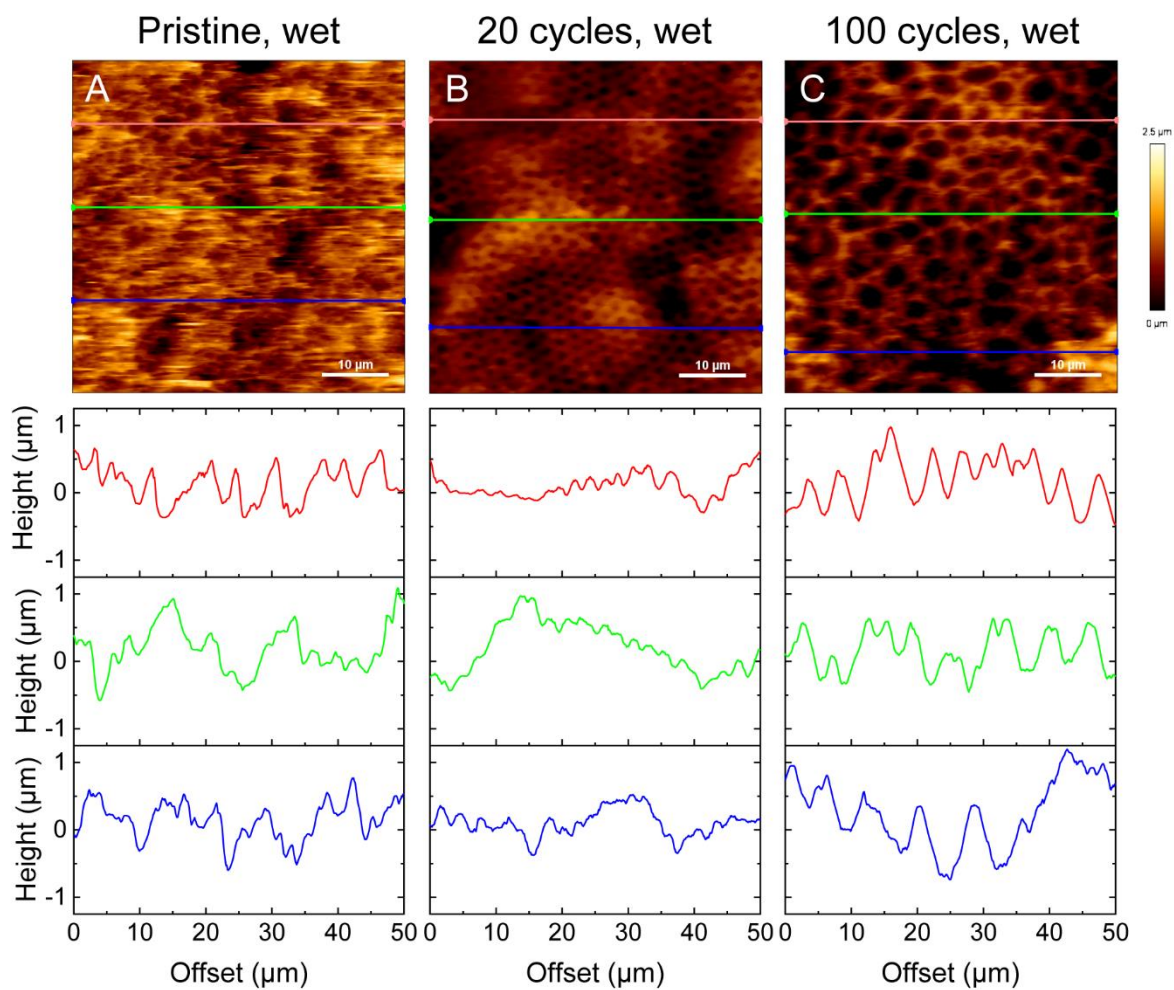
Figure S20. AFM micrographs of PEDOT-Phos films on ITO, submerged in PBS ("wet"), (A) before CV and after (B) 20 cycles and (C) 100 cycles of CV in aqueous NaCl (0.1 M). Height profiles are given for each micrograph along the three marked lines. Scan area: 50 × 50 μm.

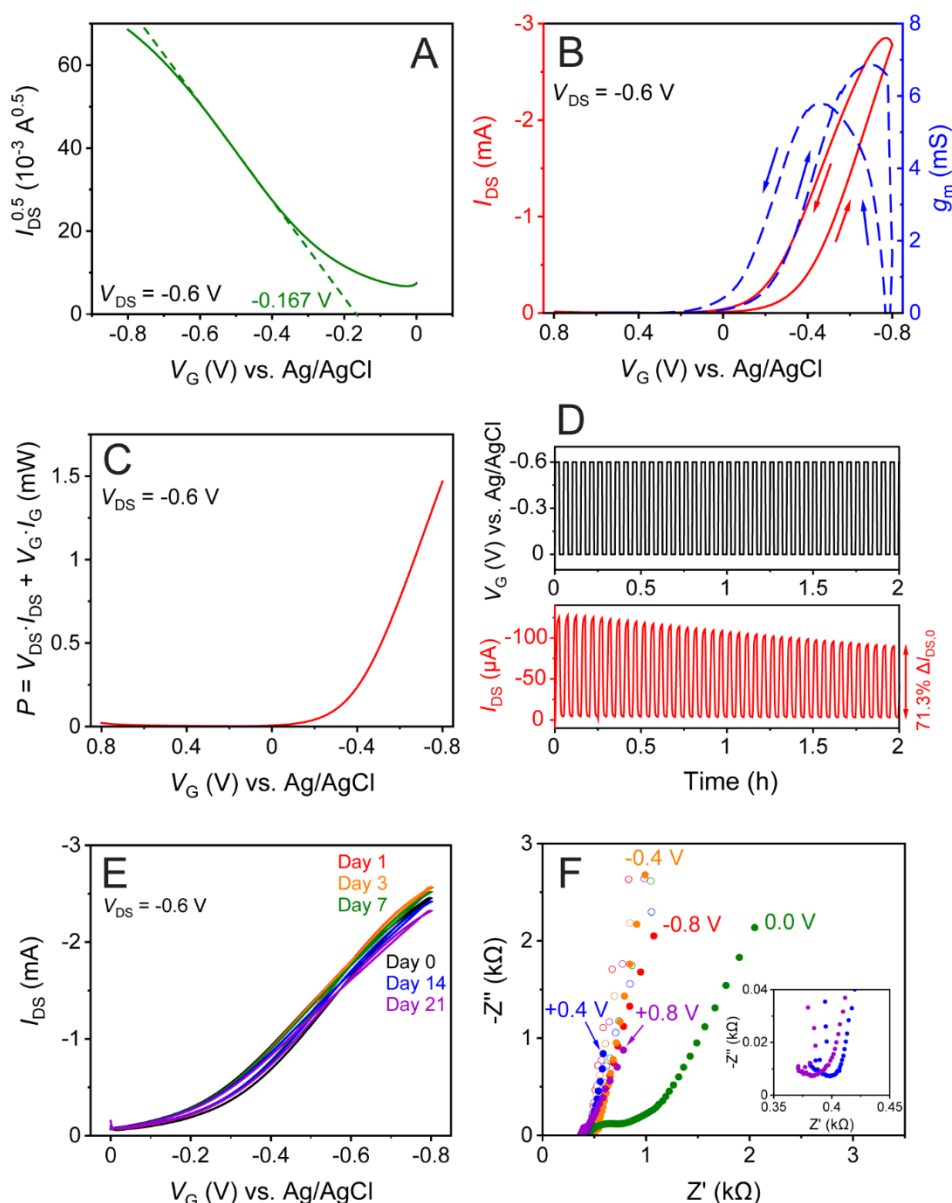## 4   *Performance in organic electrochemical transistors*

Figure S21. OECT and electrochemical measurements in aqueous NaCl (0.1 M) of a representative PEDOT-Phos film drop-cast onto an IDME. (A) Calculation of the threshold voltage V_{TH}, using data from the transfer curve recorded from 0 V to –0.8 V. V_{TH} is indicated on the plot for this specific device as –0.167 V. (B) Extended transfer curve with V_G from +0.8 V to –0.8 V. (C) Power consumption of a representative PEDOT-Phos OECT with V_{DS} = –0.6 V and V_G from +0.8 V to –0.8 V. (D) Electrochemical switching of a representative PEDOT-Phos OECT in aqueous NaCl (0.1 M) over 2 hours (40 cycles), holding each potential for 90 s. The switching times to 90% of the final response are $\tau_{90\%,ON}$ = 37.7 ± 1.4 s for doping and $\tau_{90\%,OFF}$ = 25.3 ± 0.1 s for de-doping, averaged over the first five cycles. The final magnitude of the change in I_{DS} with switching is indicated as a percentage of the original magnitude. (E) Intermittent stability of a PEDOT-Phos OECT submerged in aqueous NaCl (0.1 M) with transfer curves recorded at the indicated times after immersion. (F) Nyquist plots at various applied potentials vs. Ag/AgCl, with the inset showing more clearly the high-frequency, semicircle regime at +0.4 V and +0.8 V. A blank ITO substrate (open circle) and PEDOT-Phos film on ITO (filled circles) are shown.

Table S4. Summary of device performance parameters for PEDOT-Phos OECTs in aqueous NaCl (0.1 M). The channel dimensions are 10 μm (length) × 50 cm (width). $g_{m,max}$ = maximum transconductance; $V_{G,max}$ = gate voltage at the maximum transconductance; V_{TH} = threshold voltage; d = film thickness from profilometry; I_{ON}/I_{OFF} = on/off current ratio at V_{DS} = –0.6 V, comparing I_{DS} at –0.8 V (ON) and +0.4 V (OFF) from the extended transfer curves; C = capacitance from EIS spectroscopy at +0.4 V; $C*$ = volumetric capacitance; μ_{OECT} = charge carrier mobility. The film thickness was taken as 579 ± 73 nm, measured in the dry state.

Device	$g_{m,max}$ (mS)	$V_{G,max}$ (V)	V_{TH} (mV)	I_{ON}/I_{OFF}	C (mF)	$C*$ (F cm^{-3})	$\mu_{OECT} \times 10^5$ (cm^2 V^{-1} s^{-1})
1	8.8	–0.63	–156	594	1.25	224 ± 28	2.87
2	11.3	–0.48	–167	679	1.89	340 ± 43	3.60
3	7.7	–0.63	–162	580	1.56	281 ± 36	2.01
Avg. ± Err.*	9.3 ± 1.8	–0.58 ± 0.08	–161 ± 5	618 ± 54	1.57 ± 0.32	282 ± 62	2.83 ± 0.80

* The overall average values of $C*$ are given as average ± error calculated using error propagation. All other values with uncertainties are given as average ± standard deviation.

5 References

(1)   Garreau, S.; Louarn, G.; Buisson, J. P.; Froyer, G.; Lefrant, S. In Situ Spectroelectrochemical Raman Studies of Poly(3,4-Ethylenedioxythiophene) (PEDT). *Macromolecules* **1999**, *32* (20), 6807–6812. https://doi.org/10.1021/ma9905674.

(2)   Tran-Van, F.; Garreau, S.; Louarn, G.; Froyer, G.; Chevrot, C. Fully Undoped and Soluble Oligo(3,4-Ethylenedioxythiophene)s: Spectroscopic Study and Electrochemical Characterization. *J. Mater. Chem.* **2001**, *11* (5), 1378–1382. https://doi.org/10.1039/b100033k.

(3)   Zhao, Q.; Jamal, R.; Zhang, L.; Wang, M.; Abdiryim, T. The Structure and Properties of PEDOT Synthesized by Template-Free Solution Method. *Nanoscale Res. Lett.* **2014**, *9* (1), 1–9. https://doi.org/10.1186/1556-276X-9-557.

(4)   Xu, M.; Han, X.; Wang, T.; Li, S.; Hua, D. Conjugated Microporous Polymers Bearing Phosphonate Ligands as an Efficient Sorbent for Potential Uranium Extraction from High-Level Liquid Wastes. *J. Mater. Chem. A* **2018**, *6* (28), 13894–13900. https://doi.org/10.1039/C8TA02875C.

(5)   Smirnova, I. N.; Cuisset, A.; Hindle, F.; Mouret, G.; Bocquet, R.; Pirali, O.; Roy, P. Gas-Phase Synchrotron FTIR Spectroscopy of Weakly Volatile Alkyl Phosphonate and Alkyl Phosphate Compounds: Vibrational and Conformational Analysis in the Terahertz/Far-IR Spectral Domain. *J. Phys. Chem. B* **2010**, *114* (50), 16936–16947. https://doi.org/10.1021/jp108421c.